# Kinetics and Mechanism of the Reaction between Serum Albumin and Auranofin (and Its Isopropyl Analogue) *in Vitro*

**Jacqueline R. Roberts,[†] Jun Xiao,[†] Brian Schliesman,[†] David J. Parsons,[‡] and C. Frank Shaw, III*,[†]**

Department of Chemistry, University of Wisconsin−Milwaukee, Milwaukee, Wisconsin 53201, and Simulation Dynamics Inc., Milwaukee, Wisconsin 53211

*Received December 13, 1994*[⊗]

The first detailed kinetic analysis and mechanistic interpretation of the reactions between serum albumin and the second-generation gold drug Auranofin [$Et_3PAuSATg$ = (triethylphosphine)(2,3,4,6-tetra-*O*-acetyl-1−$\beta$-D-glucopyranosato-S-) gold(I)] and its triisopropylphosphine analogue, $i$Pr$_3$PAuSATg, *in vitro* are reported. The reactions were investigated using Penefsky spun columns and NMR saturation transfer methods. Under the Penefsky chromatography conditions with 0.4−0.6 mM albumin and a wide range of $Et_3PAuSATg$ concentrations, the reaction is biphasic. The fast phase is apparently first order in albumin with a rate constant [$k_1 = 3.4 \pm 0.3 \times 10^{-2}$ s$^{-1}$] that decreases slightly in magnitude and becomes intermediate in order at low gold concentrations, [$Et_3PAuSATg$] < [AlbSH]; it accounts for ∼95% of the Au(I) that binds. A minor, slower step [$k_2 = 2.3 \pm 0.3 \times 10^{-3}$ s$^{-1}$), which accounts for only 5% of the reaction, is also first order with respect to albumin, and zero order with respect to auranofin. For $i$Pr$_3$PAuSATg, only the first step was observed, $k_1 = (1.4 \pm 0.1) \times 10^{-2}$ s$^{-1}$, and is first order in albumin and independent of the $i$Pr$_3$PAuSATg concentration. $^{31}$P-NMR saturation transfer experiments utilizing $i$Pr$_3$PAuSATg, under equilibrium conditions, yielded second-order rate constants for both the forward ($1.2 \times 10^2$ M$^{-1}$ s$^{-1}$) and the reverse ($3.9 \times 10^1$ M$^{-1}$ s$^{-1}$) directions. A multistep mechanism involving a conformationally altered albumin species was developed. Albumin domain IA opens with concomitant Cys-34 rearrangement, allowing facile gold binding and exchange, and then closes. In conjunction with the steady-state approximation, this mechanism accounts for the different reaction orders observed under the two set of conditions. The rate-determining conformational change of albumin governs the reaction as monitored by the Penefsky columns. Rapid second order exchange of $R_3PAuSATg$ at the exposed Cys-34 residue is observed under the NMR conditions. The mechanism predicts that under physiological conditions where [$Et_3PAuSATg$] is 10−25 $\mu$M, the reaction will be second order and rapid with a rate constant of $8 \pm 2 \times 10^2$ M$^{-1}$ s$^{-1}$. The Penefsky spun columns revealed a previously unreported and novel binding mechanism, association of auranofin in the pocket of albumin−disulfide species, which was confirmed by Hummel−Dreyer gel chromatographic techniques under equilibrium conditions. This albumin−auranofin complex (AlbSSR−$Et_3PAuSATg$) is weakly bound and readily dissociates during conventional gel exclusion chromatography.

## Introduction

An estimated 5−8 million Americans are afflicted with rheumatoid arthritis (RA). Gold-based antiarthritic drugs (chrysotherapy) have been used for over 60 years in the treatment of RA with a 70% success rate. The second-generation, monomeric gold drug auranofin, AF, (2,3,4,6-tetra-*O*-acetyl-1-thio-$\beta$-D-glucopyranosato-S)(triethylphosphine)gold-(I) ($Et_3PAuSATg$) is a linear complex with phosphine ($PEt_3$) and thiolate ($^-$SATg) ligands bound to the gold(I).[1] One problem with determining the mode of action of gold-based drugs is that ligand exchange reactions occur rapidly at Au(I). When triple-labeled AF ($^{195}$Au, $^{35}$S, $^{32}$P) was injected, 82% of the gold, but only 10% of the sulfur and 42% of the phosphorus, remained in the blood after 20 min.[2] Therefore, the gold circulates as metabolites and not as the original gold complex. From 70 to 95% of the plasma gold from either AF or the first-generation injectable drugs binds to serum albumin, with the remaining gold bound primarily to globulins.[3]

Serum albumin (MW = 68 000) is the most abundant plasma protein and principle extracellular source of sulfhydryl groups in the circulatory system; it transports various substrates including metals, amino acids, hormones, fatty acids, and medicinal drugs from the site of adsorption to the site of action. Serum albumin contains 35 cysteines, of which 34 exist as disulfide bridges; the remaining cysteine residue (Cys-34) exists either as a reduced thiol in mercaptalbumin (AlbSH) or as a mixed disulfide of cysteine or glutathione (AlbSSCy, AlbSSG). The ratio of AlbSH/total Alb is ∼0.7 *in vivo*.[4] The recently reported crystal structure of several albumins established that Cys-34 lies in a fold between helices h2 and h3 of subdomain IA, where it is only partially accessible to solvent.[5] The p$K_{SH}$ of Cys-34 is ∼5.0,[6] which makes it more acidic than cysteine, glutathione, ATgSH, or $\beta$-thioglucose (TgSH), which have p$K_{SH}$ values of 8.5, 8.9, 6.4, and 7.6, respectively. Correlations of thiol affinities for gold(I) with p$K_{SH}$[7] and $\delta_P(Et_3PAuSR)$[8] suggest

[†] University of Wisconsin−Milwaukee.
[‡] Simulation Dynamics Inc.
[⊗] Abstract published in *Advance ACS Abstracts,* November 15, 1995.

(1) Hill, D. T.; Sutton, B. M. *Cryst. Struct. Commun.* **1980**, *9*, 679−686.
(2) Intoccia, A. P.; Flanagan, T. L.; Walz, D. T.; Gutzait, L.; Swagdis, J. E.; Flagiello, J.; Hwang; B. Y.-H.; Dewey, R. H.; Noguchi, H. *J. Rheumatol.* **1982**, *9*, 90−98.
(3) Herrlinger, J. D.; Alsen, C.; Beress, R.; Hecker, U.; Weikert, W. *J. Rheumatol.* **1982**, *9*, 81−89.
(4) Rosenoer, V. M.; Oratz, M.; Rothschild, M. A. *Albumin Structure, Function, and Uses*; Pergamon Press: New York, 1977; p 397.
(5) Carter, D. C.; Ho, J. X. *Adv. Protein Chem.* **1994**, *45*, 153−203.
(6) Lewis, S. D.; Misra, D. C.; Shafer, J. A. *Biochemistry* **1980**, *19*, 6129−6137.
(7) Isab, A. A.; Sadler, P. J. *J. Chem. Soc., Dalton Trans.* **1982**, 135−141.

0020-1669/96/1335-0424$12.00/0 

that Cys-34 should have a very high affinity for gold, which in turn favors the following exchange reaction:

$$\text{AlbSH} + \text{Et}_3\text{PAuSATg} \rightleftarrows \text{AlbSAuPEt}_3 + \text{HSATg} \quad (1)$$

The resulting albumin−gold complex has been well characterized by $^{31}$P-NMR,[9−12] $^{1}$H-NMR,[13,14] chromatography,[9,15] and radioisotope methods[15] and is well established.[16] It is a linear dicoordinate Au(I) complex with bond lengths of 227 pm for Au−S and 230 pm for Au−P.[9] The isopropyl and methyl analogues of auranofin ($R_3$PAuSATg, R = Me and *i*Pr) undergo similar reactions.[17,18] A structural change involving Cys-34 is required before it can form a disulfide bond or coordinate to Au(I).[14]

A second reaction (eq 2), oxidation of the phosphine moiety

$$\text{AlbSAuPEt}_3 + \text{RSH} \rightarrow \text{AlbSAuSR} + \text{Et}_3\text{PO} + \text{H}^+ \quad (2)$$

to $Et_3PO$, proceeds at a much slower rate.[19] In red blood cells, the RSH moiety can be glutathione.[20] These reactions of auranofin with serum albumin (71% of plasma protein) are critical metabolic steps, since the kinetic and thermodynamic availability of gold in circulating albumin complexes is dramatically different than that of the initial drug.

The focus of this work is the kinetic analysis of the ligand exchange reaction described in eq 1. Utilizing both chromatographic and $^{31}$P-NMR saturation transfer techniques, the rates and mechanism of $R_3$PAuSATg (R = Et, *i*Pr) binding to bovine serum albumin (BSA) were elucidated.

## Experimental Procedures

**Materials.** Bovine serum albumin (Fatty Acid Ultra Free lots DHD106, DEC106, and EHA107) was purchased from Boehringer Mannheim Biochemicals; blocked albumin (AlbSSCy) from Miles Scientific (lot 11M). 5,5′-Dithiobis(2-nitrobenzoic acid) (DTNB), 2,2′-dithiodipyridine (DTP), trimethyl phosphate (TMP), and $D_2O$ (99.8%) were all purchased from Aldrich Chemical Co. Sephadex G-25 was purchased from Sigma Chemical Co. Auranofin and $Et_3$PAuCl were generously supplied by Smith Kline and French Laboratories, *i*$Pr_3$PAuSATg and *i*$Pr_3$PAuCl by Dr. James Hoeschele. All buffers were prepared with double-distilled water and, for the measurement of Au, were sodium-free. Auranofin and *i*$Pr_3$PAuSATg was dissolved in absolute EtOH. All other chemicals were reagent grade or better.

**Protein, Sulfhydryl, and Gold Analysis.** Spectrophotometric assays were performed on Beckman DU-70 and Perkin Elmer Lambda 6 spectrophotometers. BSA concentrations were determined at $A_{278}$ ($\epsilon$ = 39 600 $M^{-1}$ $cm^{-1}$). The SH titre of BSA and ATgSH solutions was determined using either the DTP ($\epsilon_{343}$ = 7060 $M^{-1}$ $cm^{-1}$)[21] or the DTNB ($\epsilon_{414}$ = 13 600 $M^{-1}$ $cm^{-1}$)[22] methods. Gold concentrations were determined by atomic absorption spectroscopy on an IL 357 instrument. All samples analyzed (after dilution if necessary) were within a range of 0.5−6.0 $\mu$g/mL. Calibration of the instrument was performed with diluted Spex $KAu(CN)_2$ standards.

**Penefsky Column Chromatography.** Penefsky spun columns[23] were prepared by loading Sephadex G-25 resin, swelled in 0.1 M potassium phosphate buffer, pH 7.2, into 1 mL tuberculin syringes (B-D), and spinning them in a swinging bucket rotor for 30 s. The packed column was then equilibrated with three column volumes of buffer. Reaction mixtures (described below) were loaded onto the column and spun. The time required for mixing the reactants and completing the elution is typically 15−20 s. The eluants were removed and analyzed for Au via atomic absorption spectroscopy, and for BSA via its absorbance at 278 nm.

**Gel Filtration Chromatography.** Following the method of Hummel and Dreyer,[24] the reaction products were also analyzed under equilibrium conditions, with a gel filtration column preequilibrated with $Et_3$PAuSATg. Over a Sephadex G-100 column (1.5 × 50 cm), equilibrated with 0.500 mM auranofin in 0.10 M ammonium bicarbonate, pH 7.9, and 10% MeOH at 4 °C, was passed 1.0 mL of 0.500 or 0.250 mM Alb that was eluted with the same buffer. The fractions were analyzed for both gold and serum albumin.

**Kinetics of $R_3$PAuSATg (R = Et or *i*Pr) Binding to Albumin via Penefsky Chromatography.** Binding rates as a function of $R_3$PAuSATg concentrations were measured using Penefsky spun columns with reaction mixtures containing 0.600 or 0.440 mM Alb, in 0.10 M potassium phosphate buffer, pH 7.2, at 21 ± 3 °C. The reaction was initiated by adding various amounts of $R_3$PAuSATg (see figure captions and tables for final concentrations used). At 30, 45, 60, 90, 150, 300, 600, and 1800 s, aliquots (100 $\mu$L) were removed and analyzed for Au and BSA. Each reaction was repeated at least three times, with the reported data representing the mean ± standard deviation.

The corresponding rate constants were calculated by two different methods. The first method utilized an exponential fit program that employs a nonlinear least-square fitting routine based on the Marquardt algorithm.[25] The data were also treated according to standard first order [$\ln(A_\infty - A_t)$ vs time] and second order ($1/A$ vs time; $(1/([B_o] - [A_o]) \ln([A_o][B_t]/[B_o][A_t])$ vs time] kinetic relationships.[26] In the cases where the reaction was found to be biphasic, the slower phase was subtracted from the faster phase prior to calculating the rate constant of the latter.[26]

**$^{31}$P-NMR Saturation Transfer Studies.** A Bruker WM 250 spectrometer operating at 101.2 MHz for phosphorus 31, with 4 kilobit A/D conversion and quadrature phase detection over a spectral width of 10 ppm was used. The chemical shifts are reported relative to TMP as zero ppm. $D_2O$ was used as an internal lock, and the temperature was 25 °C.

A "DANTE" sequence pulse[27] was used to selectively saturate the AlbSAu*i*$Pr_3$ (68.4 ppm) and *i*$Pr_3$PAuSATg (66.2 ppm) resonances. Four parallel FIDs were acquired in an eight-scan turn to avoid the effect of any possible condition changes during the long run:

$$\{[\text{RD}-\text{DANTE}\ (t,\omega_1)-\text{observation pulse}]_8$$

$$[\text{RD}-\text{DANTE}\ (t,\omega_2)-\text{observation pulse}]_8$$

$$[\text{RD}-\text{DANTE}\ (t,\omega_3)-\text{observation pulse}]_8$$

$$[\text{RD}-\text{DANTE}\ (t,\omega_4)-\text{observation pulse}]_8\}_n$$

where RD is a delay, $t$ is the duration of the DANTE pulse, and RD + $t$ was always greater than 5-times the longer $T_1$ of *i*$Pr_3$PAuSATg[28] or


(8) Shaw, C. F., III; Coffer, M. T.; Klingbeil, J.; Mirabelli, C. K. *J. Am. Chem. Soc.* **1988**, *110*, 729−734.
(9) Coffer, M. T.; Shaw, C. F., III; Eidsness, M. K.; Watkins, J. W.; Elder, R. C. *Inorg. Chem.* **1986**, *25*, 333−339.
(10) Xaio, J.; Shaw, C. F., III *Inorg. Chem.* **1992**, *31*, 3706−3710.
(11) Malik, N. A.; Sadler, P. J. *J. Biochem. Soc. Trans.* **1979**, *7*, 731−732.
(12) Razi, M. T.; Otiko, G.; Sadler, P. J. *ACS Symp. Ser.* **1983**, *No. 209*, 371−384.
(13) Dhubhghaill, O. M. N.; Sadler, P. J.; Tucker, A. J. *J. Am. Chem. Soc.* **1992**, *114*, 1118−1120.
(14) Christodoulou, J.; Sadler, P. J.; Tucker, A. J. *Eur. J. Biochem.* **1994**, *225*, 363−368.
(15) Ecker, D. J.; Hempel, J. C.; Sutton, B. M.; Kirsch, R.; Crooke, S. T. *Inorg. Chem.* **1986**, *25*, 3139−3143.
(16) Shaw, C. F., III *Comments Inorg. Chem.* **1989**, *8*, 233−267.
(17) Shaw, C. F., III; Isab, A. A.; Hoeschele, J. D.; Starich, M.; Locke, J.; Schulteis, P.; Xiao, J. *J. Am. Chem. Soc.* **1994**, *116*, 2254−2260.
(18) Isab, A. A.; Shaw, C. F., III; Hoeschele, J. D.; Locke, J. *Inorg. Chem.* **1988**, *27*, 3588−3592.
(19) Coffer, M. T.; Shaw, C. F., III; Hormann, A. L.; Mirabelli, C. K.; Crooke, S. T. *J. Inorg. Biochem.* **1987**, *30*, 177−187.
(20) Shaw, C. F., III; Isab, A. A.; Coffer, M. T.; Mirabelli, C. K. *Biochem. Pharmacol.* **1990**, *40*, 1227−1234.
(21) Grassetti, D. R.; Murray, J. R. *Arch. Biochem. Biophys.* **1967**, *119*, 41−49.
(22) Ellman, G. L. *Arch. Biochem. Biophy.* **1959**, *82*, 70−77.
(23) Penefsky, H. S. *J. Biol. Chem.* **1977**, *252*, 2891−2899.
(24) Hummel, J. P.; Dreyer, W. J. *Biochem. Biophys. Acta* **1962**, *63*, 530−532.
(25) Bevington, P. R. *Data Reduction and Error Analysis for the Physical Sciences*; McGraw-Hill Book Co.: New York, 1969; pp 235−240.
(26) Espenson, J. H. *Chemical Kinetics and Reaction Mechanisms*, McGraw-Hill Book Co:, New York, 1981, p 218.

AlbSAuP*i*Pr$_3$ (1.1 s); $n$ is the repeat time and 8$n$ gives total number of scans acquired for each spectrum; $\omega$ is the carrier frequency; and $\omega_1$ and $\omega_3$ were set to selectively saturate the resonances of AlbSAuP*i*Pr$_3$ and *i*Pr$_3$PAuSATg. $\omega_2$ and $\omega_4$ were set at 64.2 and 70.5 ppm, respectively, to obtain the control spectra. Typically, the duration of the DANTE pulse, $t$, was 5.4 s and RD was 2 s. A total of 1600 scans was accumulated.

The apparent longitudinal relaxation rates ($1/T_{1app}$)[29] of the *i*Pr$_3$-PAuSATg and AlbSAuP*i*Pr$_3$ were measured by the selective saturation−recovery method[30,31] with a DANTE pulse to selectively presaturate the designated resonance:

$$\{[\text{RD=DANTE}\ (t,\omega_1)-\ \text{VD}(\tau)-\text{observation pulse}]_8$$

$$[\text{RD}-\text{DANTE}\ (t,\omega_3)-\text{VD}(\tau)-\text{observation pulse}]_8\}_n$$

where VD is a variable delay during which recovery occurs. Six spectra (six $\tau$ values) were acquired for each carrier frequency in an eight-scan turn shuttling between two carrier frequencies in the order of short $\tau$ to long $\tau$ values. $\omega_1 = 68.4$ ppm, $\omega_3 = 66.3$ ppm , $t = 5.4$ s, and $8n = 1600$. The proton decoupling was turned on only during the acquisition time period.

Since there is a chemical exchange involving the resonances at 68.4 and 66.3 ppm, their longitudinal magnetization recovery (designated as $T^{A}_{1app}$) reflects both "spin−lattice" relaxation and chemical exchange. Using eq 3 and a curve-fitting program (Peakfit), $T^{A}_{1app}$ values

$$M_\tau = M_0\{1 - \exp(-(\tau/T^{A}_{1app}))\} \tag{3}$$

were obtained from the $M_\tau$ vs $\tau$ curves.

**Thiol Ligand Exchange Rates.** AlbSAuP*i*Pr$_3$ was made *in situ* by mixing 40.0 $\mu$L of 77.8 mM *i*Pr$_3$PAuCl (in MeOH) with 2.0 mL of 3.01 mM BSA (SH titer 0.62, $NH_4HCO_3$ buffer, pH 7.9, 30% $D_2O$). ATgSH (60.0 $\mu$L of 107.8 mM or higher concentration in MeOH) was then added into the AlbSAuP*i*Pr$_3$ solution to create an equilibrium system for the study of the thiol ligand exchange via $^{31}$P-NMR saturation transfer (and $T_{1app}$) measurements.

The pseudo-first-order forward rate constant, $k_3^{obs}$, was calculated using eq 4,[32] where $M^{B}_{O}$ is the peak height of the *i*Pr$_3$PAuSATg

$$k_3^{obs} = \frac{1}{T^{B}_{1app}}\left[1 - \frac{M^{B}_{S}}{M^{B}_{O}}\right] \tag{4}$$

resonance in the control spectrum (with carrier frequency $\omega_4$, 64.1 ppm) and $M^{B}_{S}$ is from the spectrum following saturation of AlbSAuP*i*Pr$_3$ (with carrier frequency $\omega_1$, 68.4 ppm); $T^{B}_{1app}$ is the longitudinal relaxation time of *i*Pr$_3$PAuSATg measured by the selective saturation−recovery method. By using $M^{A}_{O}$ and $M^{A}_{S}$ [the peak heights of the AlbSAuP*i*Pr$_3$ resonance in the control spectra (with carrier frequency $\omega_2$, 70.5 ppm) and in the spectra following saturation of *i*Pr$_3$PAuSATg (with carrier frequency $\omega_3$, 66.3 ppm), respectively] and $T^{A}_{1app}$ (the longitudinal relaxation time of AlbSAuP*i*Pr$_3$ measured by selective saturation−recovery method), $k_{-3}^{obs}$ was calculated by analogy to eq 4.

Second-order rate constants, $k_4$ and $k_{-4}$, were obtained from the plots of $k_3^{obs}$ vs $[\text{AlbSH}]_{eq}$ (the equilibrium concentration of AlbSH) and $k_{-3}^{obs}$ vs $[\text{HSATg}]_{eq}$ (the equilibrium concentration of HSATg), respectively. $[\text{HSATg}]_{eq}$ and $[\text{AlbSH}]_{eq}$ were calculated from the initial concentrations, $[\text{HSATg}]_O$ and $[\text{AlbSH}]_O$:

$$[\text{HSATg}]_{eq} = [\text{HSATg}]_O - [i\text{Pr}_3\text{PAuSATg}]_{eg}$$

$$[\text{AlbSH}]_{eq} = [\text{AlbSH}]_O - [\text{AlbSAuP}i\text{Pr}_3]_{eq}$$

$[\text{AlbSAuP}i\text{Pr}_3]_{eq}$ and $[i\text{Pr}_3\text{PAuSATg}]_{eq}$ were calculated from the peak heights, $M^{A}_{O}$ and $M^{B}_{O}$, and the total concentration of gold complexes, $[i\text{Pr}_3\text{PAuCl}]$:

$$[\text{AlbSAuP}i\text{Pr}_3]_{eq}/[i\text{Pr}_3\text{PAuSATg}]_{eq} = \text{M}_\text{O}\text{A}/\text{M}_\text{O}\text{B}$$

$$[\text{AlbSAuP}i\text{Pr}_3]_{eq} + [i\text{Pr}_3\text{PAuSATg}]_{eq} = [i\text{Pr}_3\text{AuCl}]_O$$

**Computer Modeling Procedures.** The Extend simulation platform (Imagine That, Inc., San Jose, CA) was used on a Macintosh Powerbook 170. Extend has generous plotting and animation capabilities and allows the user to define "computer objects" which serve as an interface for specifying the model parameters. To model the kinetic studies, two simulation objects were developed: a "solution" object that defines the initial state of the chemical species in each experiment and a "reaction" object which defines the chemical changes and their rates. Extend then executes a defined series of steps in which the concentration changes due to elementary chemical reactions (combination, dissociation, etc.) are calculated based on the quantities at the end of the prior step and the rate constants defined for each experiment.

The chromatography studies were modeled using data from four reactions with initial concentrations (solution objects) [AlbSH] = 0.24 mM, [*AlbSH] = 0.024 mM, [AlbSAuPR$_3$] = [ATgSH] = 0, and [R$_3$-PAuSATg] = 0.8−3.0 mM. The NMR studies were modeled using data from four reactions with $[\text{AlbSH}]_o = 1.56$ mM, [*AlbSH] = 0.156 mM, [AlbSAuPR$_3$] = 0; and [R$_3$PAuSATg] = 1.47 mM, and [ATgSH] = 1.6−44 mM. The conformationally altered albumin, *AlbSH, is described in the Discussion.

## Results

In preliminary studies, the separation of free and albumin-bound gold was effected by eluting small (1 × 15 cm) gel exclusion chromatography columns under gravity flow and by ultrafiltration through 30 000 molecular weight cutoff membranes using centrifugal force.[33,34] Results from both methods consistently indicated that the reaction of serum albumin with auranofin proceeds with an apparent half-life of less than 1−2 min. However, our ability to precisely determine the rate constants and the reaction mechanism were precluded because the minimum times to effect a separation (1 min for centrifugal ultrafiltration and 2 min for gel chromatography) were longer than the half-life of the reaction. (I) is diamagnetic and also lacks UV−visible absorptions which can be monitored against a protein background. Therefore we selected Penefsky spun columns and $^{31}$P-NMR saturation transfer studies to examine the reaction rates and to elucidate the mechanism of the reaction.

**Penefsky Spun Column Chromatography**. Penefsky spun columns use a gel filtration resin and centrifugal force to rapidly and efficiently separate a macromolecule and anything bound to it from low molecular weight species.[23] Using this method, protein-bound and free gold can be separated in ∼15−20 s including sampling time. The Penefsky columns were tested (Table 1). Gold eluted in the initial eluant and the first wash if and only if it was bound to albumin. In the absence of protein, auranofin did not elute in these two fractions. Therefore, by removing and analyzing aliquots of the reaction mixture at various time points, the rate of Au binding to BSA could be accurately determined via this technique. It is much faster than

(27) Morris, G. A.; Freeman, R. *J. Magn. Reson.* **1978**, *29*, 433.
(28) RD + $t$ was always greater than 15 s, which is 5$T_1$ for *i*Pr$_3$PAuSATg in methanol, which in turn should be larger than the value in the viscous 3 mM albumin solution.
(29) $T_{1app}$ depends on both the true $T_1$ value and the exchange phenomenon under observation. Furthermore, it must be measured in the protein solution under study, not in a simple aqueous solution, because the viscosity of the protein solution affects $T_1$. Thus, the similarity of the values for the protein and low molecular weight complexes are not unexpected.
(30) Markley, J. L.; Horsley, W. H.; Klein, M. P. *J. Chem. Phys.* **1971**, *55*, 3604.
(31) Tropp, J. *Biochemistry* **1981**, *20*, 2133.
(32) Krishna, N. R.; Huang, D. H.; Glickson, J. D.; Brown, R.; Walter, R. *Biophys. J.* **1979**, *26*, 345.
(33) Schliesman, B. D. M.S. Thesis, University of Wisconsin−Milwaukee, Milwaukee, WI, 1991.
(34) Roberts, J. R. Ph.D. Dissertation, University of Wisconsin−Milwaukee, Milwaukee, WI, 1993.

**Table 1.** Penefsky Spun Column Separations of Albumin-Bound and "Free" Gold Species[a]

| applied | | recovered (%)[b] | |
|---|---|---|---|
| albumin ($\mu$M) | gold ($\mu$M) | albumin ($\mu$M) | gold ($\mu$M) |
| 600 | | 580 (97) | |
| | 151 | | 4 (3) |
| | 4000 | | 7 (0.2) |
| 600 | 151[c] | 610 (102) | 156 (103) |
| 600 | 151[d] | 623 (103) | 100 (66) |

[a] 100 mM potassium phosphate, pH 7.2; reactions were initiated by adding $Et_3PAuSATg$ to albumin. Aliquots of 100 $\mu$L were loaded onto a spun column. Each sample was spun and washed with 50 $\mu$L of buffer. The albumin concentration was determined by $A_{278}$ and the Au concentration was determined by atomic absorption spectroscopy. [b] Initial eluant and first wash. [c] A 30 min incubation. [d] A 45 s incubation.

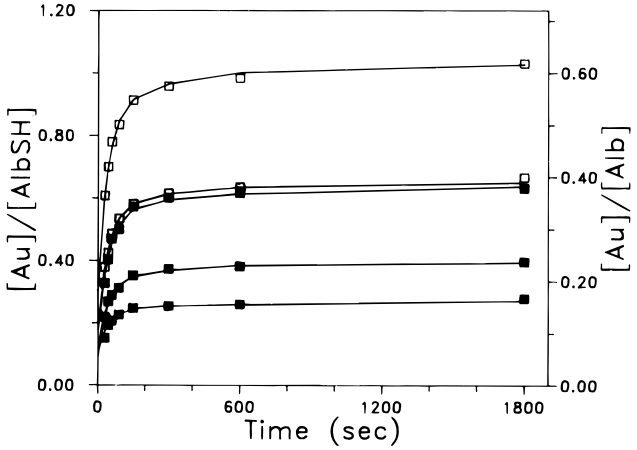


**Figure 1.** Kinetics of gold(I) binding when $[Et_3PAuSATg]_o < [AlbSH]_o$. All reactions were performed in 0.100 M potassium phosphate buffer, pH 7.2, with either (■) 0.600 mM Alb (0.372 mM AlbSH) or (□) 0.440 mM Alb (0.272 mM AlbSH). $[Et3PAuSATg]_o$ for the reactions was 0.093, 0.151, 0.225, 0.188, and 0.300 mM. The solid lines are the data generated from the best-fit nonlinear program.

the conventional column chromatography and membrane-based rapid centrifugation techniques tried initially.

**Rates of $Et_3PAuSATg$ and *i*$Pr_3PAuSATg$ Binding to Albumin.** The rate of binding of Au(I) to albumin (eq 1) as a function of Au(I) concentrations was determined utilizing the Penefsky spun columns. When the concentration of auranofin is less than that of mercaptalbumin, the reaction goes to completion based on gold concentration. In all cases, at least 90−95% of the reaction was completed within 90 s.

To determine the rate constant(s) for each reaction, the data were analyzed using a nonlinear least-squares, best-fit program.[25] The two first order rate constants determined are listed in Table 2, and the curves generated by this analysis are the solid lines in Figure 1. To corroborate these rate constants, standard methods of analysis for first- and second order fits were also employed. Each set of data was plotted as a function of $\ln(A_\infty - A_t)$ vs time, as 1/A vs time, and as $(1/[B_o] - [A_o])\ln([A_o][B_t]/[B_o][A_t])$ vs time.[26] When the relationships for second order processes (i.e., $[A]^2$ and [A][B]) were plotted, curved lines were obtained, thus ruling out a second order rate constant. However, the data were found to have two linear regions when analyzed by the first-order relationship, $\ln(A_\infty - A_t)$ vs time. Rate constants for the fast phase ($k_1^{obs}$; $t \leq 90$ s, after correcting for the slow phase), and the slow phase ($k_2^{obs}$; $t > 90$ s) were determined by standard algorithms.[26] The $R^2$ values from the first order plots for both the fast phase ($k_1$; $t \leq 90$ s) and slow phase ($k_2$; $t > 90$ s) were consistently much closer to 1 than were the values obtained using the second order plots. The

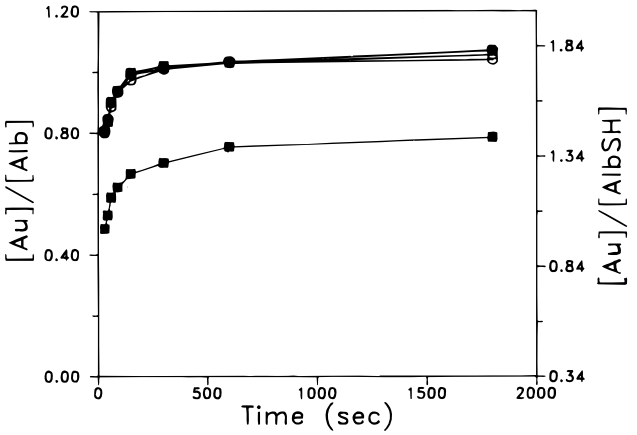


**Figure 2.** Kinetics of gold(I) binding under pseudo-first-order conditions. All reactions were run with 0.400 mM Alb (0.260 mM AlbSH) in the presence of a pseudo-first order excess of auranofin, (○) 3.00 mM, (●) 2.46 mM, (□) 1.38 mM, or a slight excess (■) 0.30 mM. The data are plotted as the ratio of Au(I) to total albumin vs time. The solid lines represent the data generated from the best-fit nonlinear kinetic program. Other conditions as described in Figure 1.

rate constants obtained by the best-fit program and by standard methods were in good agreement.

When the reaction was run with a pseudo-first order excess (7−11-fold) of auranofin, the values of the observed rate constants, $k_1^{obs}$, were independent of the gold concentration (Table 2 and Figure 2). When the observed rate constants, $k_1^{obs}$, were plotted as a function of Au concentration, the slope was indistinguishable from zero, thus demonstrating that under these conditions the rate of the fast phase is first order with respect to serum albumin and zero order with respect to auranofin (eq 5). The slow step was typically only ~5% of the reaction, but

$$\text{rate}_f = k_1[\text{albumin}] \quad (5)$$

the $k_2^{obs}$ values are reproducible (Table 2). Like the fast-phase rate constants, they are independent of the Au concentration. Therefore, this phase also has a first order dependence on the serum albumin concentration, eq 6. For $Et_3PAuSATg$, the

$$\text{rate}_s = k_2[\text{albumin}] \quad (6)$$

average rate constants obtained from the standard first-order plots for $k_1$ and $k_2$ are $(3.4 \pm 0.3) \times 10^{-2}$ and $(2.3 \pm 0.3) \times 10^{-3}$ $s^{-1}$, respectively, and fall within experimental error of the rates obtained from the best-fit program.

The auranofin analogue, $iPr_3PAuSATg$, reacts analogously to eq 1, to form an albumin−gold−phosphine complex.[17] The kinetics of the reaction were also examined and only a single reaction phase was observed (Table 2). The observed rate constants are also independent of the gold concentration and similar to $k_1^{obs}$ for auranofin. They have an average value of $(1.4 \pm 0.1) \times 10^{-2}$ $s^{-1}$. Thus, the $iPr_3PAuSATg$ reaction and the faster, dominant phase for $Et_3PAuSATg$ have first-order, albumin-dependent rate laws and similar rate constants.[35]

**Auranofin Binding to Albumin Cys-34 Disulfides (Alb-SSR).** When excess AF was employed, an unexpected stoi-

(35) The fact that the $k_1$ values for $Et_3PAuSATg$ and $iPr_3PAuSATg$ differ by only a factor of 2 strongly suggests that they are governed by the same process on albumin and entail, at most, only minor perturbations caused by the differences in the two phosphine ligands. A speculative explanation for this 2-fold variation in rate, offered at the request of a reviewer, and consistent with the mechanism of eqs 11−13, is that the extent of the protein breathing motions that open the protein to expose Cys-34 to solvent may vary from event to event and, consequently, discriminate against the larger *i*$Pr_3PAuSATg$. This in turn would give rise to a marginally smaller rate constant.

**Table 2.** Observed Rate Constants for $R_3PAuSATg$ Albumin Reaction[a]

| $[Alb]_O$ ($\mu$M) | $[AlbSH]_O$ ($\mu$M) | $[Et_3PAu\text{-}SATg]_O$ ($\mu$M) | $[i Pr_3PAu\text{-}SATg]_O$ ($\mu$M) | $10^2 k_1^{obs}$ ($s^{-1}$) | $10^3 k_2^{obs}$ [b] ($s^{-1}$) |
|---|---|---|---|---|---|
| 600 | 360 | 93 | | 3.0 ± 0.6 | 1.9 ± 0.8 |
| 600 | 360 | 151 | | 2.7 ± 0.2 | 2.3 ± 0.8 |
| 600 | 360 | 225 | | 2.6 ± 0.3 | 2.3 ± 0.4 |
| 440 | 265 | 188 | | 3.2 ± 0.7 | 2.1 ± 0.8 |
| 440 | 265 | 300 | | 3.2 ± 0.4 | 2.4 ± 0.8 |
| 400 | 240 | 300 | | 3.5 ± 0.4 | 3.1 ± 0.1 |
| 400 | 240 | 840 | | 3.3 ± 0.1 | 2.4 ± 0.3 |
| 400 | 240 | 1200 | | 3.5 ± 0.1 | 2.4 ± 0.7 |
| 400 | 240 | 1380 | | 3.2 ± 0.5 | 3.1 ± 0.3 |
| 400 | 240 | 1920 | | 3.3 ± 0.4 | 2.4 ± 0.9 |
| 400 | 240 | 2460 | | 3.4 ± 0.5 | 2.1 ± 0.4 |
| 400 | 240 | 3000 | | 3.4 ± 0.4 | 2.1 ± 0.6 |
| 420 | 250 | | 2190 | 1.5 ± 0.3 | *c* |
| 420 | 250 | | 2730 | 1.4 ± 0.2 | *c* |
| 420 | 250 | | 3110 | 1.6 ± 0.4 | *c* |
| 420 | 250 | | 4200 | 1.4 ± 0.1 | *c* |

[a] Reactions were carried out in 0.10 M potassium phosphate buffer, pH 7.2, at 21 °C. Aliquots were removed periodically and the protein-bound gold was measured by AAS (Au) and UV−visible spectrometry (albumin) after separation over a Penefsky spun column. [b] Because the rate constant $k_1^{obs}$ accounts for 95% (or more than 4 half-lives) of the reaction, it would be acceptable to ignore the residual 5% of the reaction. However, it is observed consistently with rate constants of $k_2^{obs} = (1.9-3.1) \times 10^{-3}$ and consists of 4−7% of the reaction, suggesting that it is a reproducible phenomenon. Its contribution to the overall reaction is too small (4−8%) to be the weaker binding observed by the Penefsky columns (~30% of the BSA), but it could (1) represent a movement of the $Et_3PAu^+$, with or without ATgSH bound, from weaker to stronger binding sites on albumin, (2) result from ATgSH reduction of Cys-34 disulfide bonds to generate additional AlbSH, (3) be related to the conformational change of Cys-34 reported by Christodoulou et al.,[14] or (4) result from reaction with a minor constituent of albumin, which is a microheterogeneous mixture.[4,5] [c] Not observed.

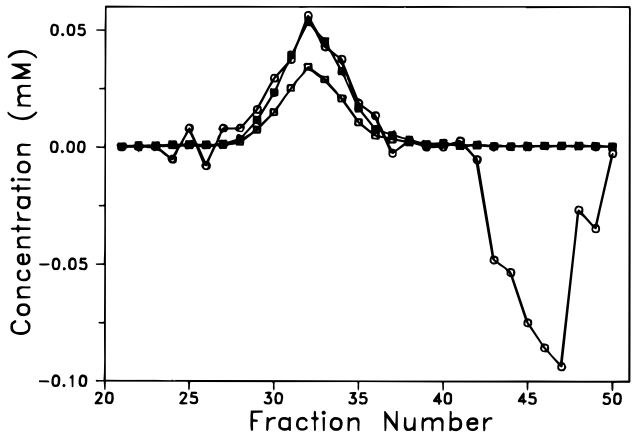


**Figure 3.** Hummel−Dreyer gel filtration[24] profile of the equilibrium binding between auranofin and serum albumin. A 1.0 mL sample of a 500 $\mu$M serum albumin (320 $\mu$M AlbSH) was loaded onto a Sephadex G-100 (1.5 × 50 cm) column preequilibrated in 500 $\mu$M $Et_3PAuSATg$ in 0.10 $NH_4HCO_3$, pH 7.9, and 10% MeOH and eluted with the same buffer at a flow rate of 15−20 mL/h. The $AlbSAuPEt_3$ complex eluted in fractions 29−36, and the inverse gold peak at fractions 40−53: (○) [Au]; (■) [Alb]; (□) [AlbSH]. The AlbSH concentration was calculated as $[Alb_{TOT}]$ × SH titer for comparison with the extent of gold binding. The concentration of gold bound to serum albumin was equivalent to the $Alb_{TOT}$, not the mercaptalbumin concentration. A similar profile was observed when the serum albumin concentration was decreased to 250 $\mu$M.

chiometry was obtained: the albumin-bound gold increased until each BSA molecule contained one gold (Figure 2, secondary axis): $Au/Alb_{TOT} = 1.00 \pm 0.05$. That is, the gold bound exceeded the mercaptalbumin present (Figure 2, primary axis). This phenomenon has been observed only with the Penefsky column data. Previously reported conventional gel filtration studies,[9,15,34] with gold in excess of albumin, consistently found that the Au binding ability is equivalent to the mercaptalbumin concentration ($Au/Alb_{TOT}$ = SH titer). We are able to reproduce these earlier results when the albumin and auranofin preparations from the Penefsky column studies are resolved on a conventional column. Thus, the Penefsky column stoichiometry (1 Au/$Alb_{TOT}$) suggests that all of the Au was associated with and saturated a single site, the Cys-34-containing crevice of serum albumin, regardless of whether Cys-34 is in the mercaptalbumin or disulfide forms. Binding at a different site, such as the drug sites in domains IIA or IIIA[4,5,36] in addition to binding at Cys-34, is precluded because it would yield an $Au/Alb_{TOT}$ ratio of ~1.6, not 1.0 as observed here. The difference between the conventional and Penefsky gel filtration experiments is that the former are slow, thus allowing dissociation of the $R_3PAuSATg$ from the disulfide forms of albumin, while the Penefsky columns are eluted rapidly and labile adducts can be observed. In both cases, the $Et_3PAu^+$ moiety bound at Cys-34 according to eq 1 is retained.

To confirm this novel binding to the albumin disulfides, equilibrium gel filtration columns, as described by Hummel and Dreyer,[24] were run (Figure 3). The gel filtration column is preequilibrated with and then eluted with an auranofin-containing buffer. This method prevents weakly bound auranofin from dissociating during the chromatographic process. A positive gold peak equivalent to the amount of gold bound at equilibrium should elute with albumin, and a second negative peak should elute after the $AlbSAuPEt_3$ peak. The background will be the buffer gold concentration. Exactly the anticipated result is shown in Figure 3: the ratio of protein-bound gold to total albumin was 1:1. Thus, the interaction of gold and the non-mercaptalbumin species AlbSSR (RS = Cys or GS) can be described by eq 7, in which there is equilibrium binding of

$$AlbSSR + Et_3PAuSATg \rightleftharpoons AlbSSR\text{−}Et_3PAuSATg \quad (7)$$

auranofin at the Cys-34 disulfide sites of albumin. During passage over the longer, conventional gel columns, the AlbSSR−$Et_3PAuSATg$ complex dissociates and the gold then elutes with the low molecular weight fractions. During the Hummel−Dreyer chromatography, excess gold in the eluting buffer keeps the site saturated. The Penefsky columns are eluted so rapidly that dissociation cannot occur during passage over the column, and they produce the same result as the Hummel−Dreyer method. The results demonstrate for the first time that $Et_3PAuSATg$ can bind hydrophobically in the AlbSSCy pocket. Dhubhghaill *et al.* have previously reported hydrophobic binding of the free ATgSH ligand to albumin.[13]

(36) He, X. M.; Carter, D. C. *Nature* **1992**, *358*, 209−215.

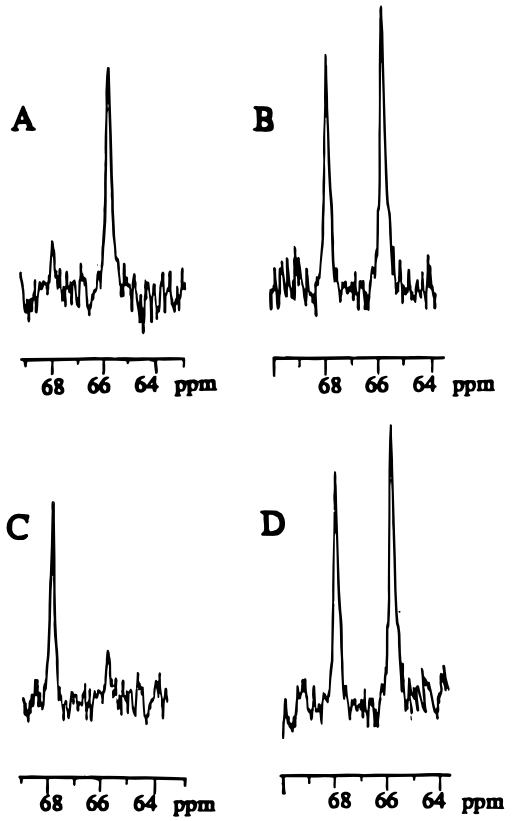


**Figure 4.** $^{31}$P-NMR spectra (101.3 MHz) of the reaction mixture of AlbSAuPiPr$_3$ and ATgSH. Selective saturation was applied on the carrier frequencies ($\omega$): (A) 68.4 ppm (AlbSAuP*i*Pr3); (B) 64.1 ppm (control for A); (C) 66.3 ppm (*i*Pr$_3$PAuSATg); and (D) 70.5 ppm (control for C). The intensities $M_O^A$ (68.4 ppm) and $M_O^B$ (66.3 ppm) were measured from (D) and (B), respectively, which were not affected by the selective saturation. The intensities, $M_S^B$ (66.3 ppm) and $M_S^A$ (68.4 ppm) were measured from (A) and (C), respectively, in which, the selective saturation of one resonance decreased the other resonance. Conditions: 3.0 mM albumin (SH titer, 0.62); 100 mM $NH_4HCO_3$ buffer, pH 7.9, 30% $D_2O$; [Au] = 1.5 mM.

**$^{31}$P-NMR Saturation Transfer Studies.** To investigate further the albumin−auranofin binding reaction (eq 1), we used $^{31}$P-NMR saturation transfer experiments under equilibrium conditions. In this method, the magnetization of a specific nucleus on one species is perturbed with an irradiating pulse and the rate of magnetization transfer to another species in equilibrium with it is determined. Application of this technique to the thiol exchange of auranofin, eq 1, was complicated by the progressive formation of $Et_3PO$ (eq 2) during the long acquisition times required for these experiments. This decreases the concentration of the $Et_3$PAuSATg and AlbSAuP$Et_3$ species. Therefore, we substituted *i*Pr$_3$PAuSATg, which undergoes thiol exchange, eq 8,[17] analogous to eq 1, but does not readily

$$\text{AlbSH} + i\text{Pr}_3\text{PAuSATg} \underset{k_{-3,\text{obs}}}{\overset{k_{3,\text{obs}}}{\rightleftharpoons}} \text{AlbSAuP}i\text{Pr}_3 + \text{HSATg} \quad (8)$$

generate *i*Pr$_3$PO by a process analogous to eq 2.[17] From previous studies, the resonances of *i*Pr$_3$PAuSATg and AlbSAuP*i*Pr$_3$ are known to be 66.3 and 68.4 ppm, respectively.[17]

Figure 4 shows a typical set of $^{31}$P-NMR saturation transfer spectra. When the carrier frequency was set on the resonance of AlbSAuP*i*Pr$_3$, 68.4 ppm, or *i*Pr$_3$PAuSATg, 66.3 ppm, the DANTE presaturation pulse efficiently saturated the signal (Figure 4a,c). In the control spectra obtained with the carrier frequencies set 2 ppm on either side of the *i*Pr$_3$PAuSR (RS = AtgS and AlbS) resonances at 70.5 (Figure 4d) and 64.1 ppm (Figure 4b), respectively, the intensities of both resonances are unaffected by the presaturations. Thus, the selective saturation did not suppress the resonance 2 ppm away from the carrier frequency. Therefore, the decreases of the resonances at 68.4 ppm in Figure 4c and 66.3 ppm in Figure 4a, compared with the intensities in the control spectra, result from saturation transfer due to chemical exchange.

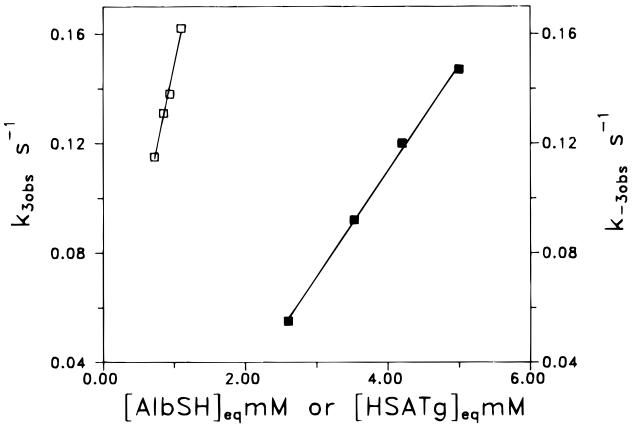


**Figure 5.** Plots of $k_3^{obs}$ vs [AlbSH]$_{eq}$ (□) and $k_{-3}^{obs}$ vs [ATgSH]$_{eq}$ (■). From the slopes, the second order constants, $k_4$ and $k_{-4}$ were determined to be $1.2 \times 10^2$ and $3.9 \times 10^1$ M$^{-1}$ s$^{-1}$, respectively. Conditions as in Figure 4.

The rate constants for the forward and reverse processes of eq 8, $k_3^{obs}$ and $k_{-3}^{obs}$, were obtained at four different concentrations of added ATgSH. The plots of $k_3^{obs}$ vs [AlbSH]$_{eq}$ and $k_{-3}^{obs}$ vs [HSATg]$_{eq}$ (Figure 5) show that these observed constants are concentration dependent. Thus, the ligand exchange process in each direction is second order: first order with respect to the gold−phosphine complex and first order with respect to thiol (eqs 9 and 10), with $k_3^{obs} = k_4$[AlbSH] and $k_{-3}^{obs}$

$$\text{rate}_f = k_4[\text{AlbSH}][i\text{Pr}_3\text{PAuSATg}] \quad (9)$$

$$\text{rate}_r = k_{-4}[\text{AlbSAuP}i\text{Pr}_3][\text{ATgSH}] \quad (10)$$

$= k_{-4}$[ATgSH]. From the slopes of the lines in Figure 5, the second order rate constants, $k_4$ and $k_{-4}$ were found equal to $1.2 \times 10^2$ and $3.9 \times 10^1$ M$^{-1}$ s$^{-1}$, respectively. As expected from the extent of reaction described previously,[9,11,15,17,37] $k_4$ is greater than $k_{-4}$.

## Discussion

Apparently disparate reaction orders and rate constants were determined using the two methods of analysis. By using the Penefsky spun columns, the reaction was found to be first order in albumin and independent of the $Et_3$PAuSATg or *i*Pr$_3$-PAuSATg concentrations. The rate constants for the two gold species are similar, $(3.4 \pm 0.3) \times 10^{-2}$ for $Et_3$PAuSATg and $(1.4 \pm 0.1) \times 10^{-2}$ for *i*Pr$_3$PAuSATg, as expected if the reaction is dependent on only the albumin concentration (Figure 2 and eqs 5 and 6).[35] The NMR result is quite different: a second-order reaction, dependent on both the albumin and *i*Pr$_3$PAuSATg concentrations was found (Figure 5 and eqs 9 and 10). The conditions for each set of reactions, however, are quite dissimilar. The Penefsky column procedure monitors the forward reaction immediately after mixing the two reactants, usually with a significant excess of gold complex, which helps to push the reaction to completion. The NMR studies require that the system be at equilibrium and that significant concentrations of each of the four species in eq 8 be present.

(37) Xiao, J. Ph.D. Dissertation, University of Wisconsin−Milwaukee, Milwaukee, WI, 1993.

Computer simulation using the program Extend was carried out in parallel with development of the mechanism described below. To successfully model both sets of reaction conditions it was necessary to define a conformationally altered (more-open) albumin, *AlbSH, which exists in dynamic equilibrium with AlbSH. For this equilibrium (AlbSH ⇌ *AlbSH), the reverse rate constant, $k_r$, must be at least 10-fold greater than the forward rate constant; $k_f = 0.034\ s^{-1}$; $k_r = 0.34\ s^{-1}$. The forward and reverse steps for reaction

$$*\text{AlbSH} + \text{R}_3\text{PAuSATg} \rightleftharpoons *\text{AlbSAuPR}_3 + \text{ATgSH}$$

were $k_f = 1.6\ mM^{-1}\ s^{-1}$ and $k_r = 0.029\ mM^{-1}\ s^{-1}$. Using these parameters, which were in good agreement with the experimental results, the rate of formation of $AlbSAuPR_3$ monitored by Penefsky chromatography and the rate of saturation transfer in the NMR experiments were reproduced. From the modeling it is clear that the chromatography examines the initial stage of the reaction, before equilibrium is reached, when the formation of *AlbSH is rate-limiting. When the reaction reaches equilibrium, however, the concentration of $R_3PAuSATg$ affects the rate of the net forward reaction, as in the NMR experiments.

A minimal mechanism that can account for the first order dependence on only albumin under the Penefsky column conditions and the second order dependence of the NMR experiments is the following:[34,37]

$$\text{AlbSH} \underset{k_{-5}}{\overset{k_5}{\rightleftharpoons}} *\text{AlbSH} \tag{11}$$

$$*\text{AlbSH} + \text{R}_3\text{PAuSATg} \underset{k_{-6}}{\overset{k_6}{\rightleftharpoons}} *\text{AlbSAuPR}_3 + \text{ATgSH} \tag{12}$$

$$*\text{AlbSAuPR}_3 \underset{k_{-7}}{\overset{k_7}{\rightleftharpoons}} \text{AlbSAuPR}_3 \tag{13}$$

*****AlbSH and *****$AlbSAuPR_3$ are conformationally altered albumin molecules in which Cys-34 is accessible to other solute molecules. Cys-34 is located in a crevice between helices h2 and h3 and estimated to be 950 pm from the albumin surface.[38] It is partially water-inaccessible.[5,36] The slow reaction of thiol reagents with Cys-34[39] indicates that one or more open conformations exist. It is necessary to postulate a closure of the open albumin after gold binding, otherwise if the Cys-34 bound $i\text{Pr}_3\text{Au}^+$ moiety were solvent-accessible, the saturation transfer from $AlbSAuPi\text{Pr}_3$ to $i\text{Pr}_3$PAuSATg would occur faster than the NMR time scale, as observed for low molecular weight thiols (e.g., penicillamine or cysteine) in equilibrium with auranofin and contrary to the observations in Figure 5. It should be noted that the forward direction of eq 13 completes a "breathing motion" of the protein and that the reverse direction of eq 13 corresponds to the forward direction of eq 11.

By applying the steady-state approximation to *****AlbSH and *****$AlbSAuPR_3$ in eqs 11−13, the following complex relationship is derived:

$$\frac{\text{d[AlbSAuPR}_3\text{]}}{\text{d}t} = k_7\left\{\frac{k_{-7}k_{-5}[\text{D}] + k_{-7}k_6[\text{B}][\text{D}] + k_5k_6[\text{A}][\text{B}]}{k_{-6}k_{-5}[\text{C}] + k_7k_{-5} + k_7k_6[\text{B}]}\right\} - k_{-7}[\text{D}] \tag{14}$$

where [A] is AlbSH, [B] is $R_3PAuSATg$, [C] is ATgSH, and [D] is $AlbSAuPR_3$.

The Penefsky column conditions with excess $R_3PAuSATg$ present favor the forward reaction since reactants are mixed in the absence of products. After eliminating terms containing the concentrations of products, all of which are negligible at the beginning of the reaction, and using the inequality $k_6[B] > k_{-5}$, which applies when $R_3PAuSATg$ is present in excess, eq 14 simplifies to eq 15.[40] Thus, rate constant $k_5$ of the

$$\frac{\text{d[AlbSAuPR}_3\text{]}}{\text{d}t} = k_5[\text{A}] \tag{15}$$

mechanism is identical to the experimental first order rate constant, $k_1$ (eq 5), determined for the forward reaction with $R_3PAuSATg$ present in excess.

The experimental NMR saturation transfer results can be derived from the same mechanism (eqs 11−13). The rate of saturation transfer from $i\text{Pr}_3$PAuSATg to $AlbSAuPi\text{Pr}_3$ will be governed by the forward step of eq 12, for which the time derivative is

$$\frac{\text{d[R}_3\text{PAuSATg]}}{\text{d}t} = k_6[\text{B}][*\text{AlbSH}] \tag{16}$$

Incorporation of the steady-state expansion yields

$$\frac{\text{d[R}_3\text{PAuSATg]}}{\text{d}t} = k_6[\text{B}]\left\{\frac{k_5k_7[\text{A}] + k_5k_{-6}[\text{A}][\text{C}] + k_{-6}k_{-7}[\text{C}][\text{D}]}{k_{-5}k_7 + k_{-5}k_{-6}[\text{C}] + k_6k_7[\text{B}]}\right\} \tag{17}$$

The assumption $k_{-5} < k_6[B]$ remains valid and the corresponding inequality, $k_7 < k_{-6}[C]$ applies, so that the expression in brackets simplifies to yield

$$\frac{\text{d[R}_3\text{PAuSATg]}}{\text{d}t} = k_6[\text{B}]\left\{\frac{k_5k_{-6}[\text{A}][\text{C}] + k_{-6}k_{-7}[\text{C}][\text{D}]}{k_{-5}k_{-6}[\text{C}] + k_6k_7[\text{B}]}\right\} \tag{18}$$

The NMR experiment employed excess ATgSH to establish the equilibrium, so that [C] ≫ [B]. Furthermore the numerator term $k_{-6}k_{-7}$[C][D] does not contribute to the saturation transfer, so after eliminating these terms and algebraically simplifying one obtains the result

$$\frac{\text{d[R}_3\text{PAuSATg]}}{\text{d}t} = \frac{k_5k_6}{k_{-5}}[\text{A}][\text{B}] \tag{19}$$

Similar arguments can be applied to the reverse process for which the result is

$$\frac{\text{d[AlbSAuPR}_3\text{]}}{\text{d}t} = \frac{k_{-7}k_{-6}}{k_7}[\text{C}][\text{D}] \tag{20}$$

Thus, the experimental second order rate constants, $k_4$ and $k_{-4}$, from the NMR saturation transfer experiments can be equated with the collections of rate constants, $k_5k_6/k_{-5}$ and $k_{-7}k_{-6}/k_7$ of the mechanism.

(38) Hull, H. H.; Chang, R.; Kaplan, L. *J. Biochim. Biophys. Acta* **1975**, *400*, 132−136.
(39) Wilson, J. M.; Wu, D.; Motiu-DeGrood, R.; Hupe, D. J. *J. Am. Chem. Soc.* **1980**, *102*, 359−363.

(40) The converse possibility, that $k_{-5}$ might in general be much larger than $k_6[B]$, can be tested against the data. The reaction would in effect be a pre-equilibrium for which the rate expression would reduce to $k_5k_6[A][B]/(k_{-5} + k_6[B])$. When $k_{-5} >> k_6[B]$, the expression reduces to $(k_5k_6/k_{-5})[A][B]$ and the Penefsky column data would be dependent upon the $R_3PAuSATg$ concentration, and not independent of it, as observed in Table 2 for both auranofin and the isopropyl analogue.

The inequality of $k_6[R_3PAuSATg] > k_{-5}$ can be tested against the experimentally determined rate constants and concentrations. According to the steady-state approximation, $k_4 = k_6k_5/k_{-5}$, and $k_1 = k_5$. Hence, the ratio $k_4[R_3PAuSATg]/k_1$ is equivalent to $k_6[R_3PAuSATg]/k_{-5}$ and should be significantly greater than one. Substitution of the $k_4$ and $[i\text{Pr}_3PAuSATg]_{eq}$ values for the NMR experiments and the Penefsky column $k_1$ value for $i\text{Pr}_3$-PAuSATg yields a ratio of ~10−20, which confirms the assumption. Since the ratio $k_5/k_{-5}$ is small (i.e., the albumin is predominantly in the closed pocket form), the inequality can be extended: $k_6[R_3PAuSATg] > k_{-5} > k_5$. The corresponding inequality for the reverse reaction is also likely: $k_{-6}[ATgSH] > k_7 > k_{-7}$. Thus, the ligand exchange process of eq 12 is much more rapid than the pocket opening, and multiple exchange events occur during each open cycle. The second-order ligand exchange process ($k_4 = k_5k_6/k_{-5}$) revealed by the NMR experiment is consistent with the rapid kinetics and associative mechanisms of ligand exchange observed with other gold(I) thiolates[7,41] but remains slow on the NMR time scale due to the contribution of the crevice-opening process ($k_5$, $k_{-5}$) to the exchange. These results are consistent with the conformational change, observed by $^1$H NMR spectroscopy, which causes the cysteine to shift to a more open environment upon gold binding.[14]

Both first- and second-order reactions were observed previously for reactions of albumin with various disulfide reagents:[39] some (e.g., DTNB and cysteamine disulfide) react by second order processes and others (e.g., dithiodiacetate), although construed not to react in the absence of a second-order rate constant, follow a slower albumin-limited first-order process.[39] These patterns are attributed in part to conformational changes of the crevice environment surrounding Cys-34.[39] Sadler *et al.*[14,42] recently postulated a rearrangement of Cys-34 preceding gold binding, which could also account for the first-order process. However, the rate and mechanism have not been determined for comparison with those reported here.

Returning to the Penefsky column results, it is surprising to note that when the auranofin concentrations are smaller than the albumin concentration (e.g., Table 2, where $[AlbSH]_o$ = 360 $\mu$M and $[Et_3PAuSATg]_o$ = 93−225 $\mu$M), the reaction remains first order and the rate constants are only slightly diminished, ~$(2.6-3.0) \times 10^{-2}$ s$^{-1}$, compared to $3.4 \times 10^{-2}$ s$^{-1}$ when auranofin is in excess. In the absence of the NMR findings of a second-order exchange at equilibrium, one would conclude that the reaction is a simple first-order reaction under all conditions. However, by using the mechanism of eqs 11−13 and omitting the assumption that $k_6[B] > k_{-5}$ from the derivation of eq 15, the result obtained is

$$\frac{d[AlbSAuPR_3]}{dt} = \frac{k_5k_6[B][A]}{k_{-5} + k_6[B]} = k_{obs}[A] \qquad (21)$$

$$k_1^{obs} = \frac{k_5k_6[B]}{k_{-5} + k_6[B]} \qquad (22)$$

When $k_6[B] \approx k_{-5}$, an intermediate order reaction with an apparent first-order rate constant will be obtained. In this region, the numerical value of $k_1^{obs}$ decreases slightly as [B] decreases. When $k_{-5} > k_6[B]$, which holds only at gold concentrations below those used in this study, the reaction becomes second order and $k_1^{obs}$ falls off rapidly. One can model the observed rate constants of Table 2, using the restraints $k_4 = k_5k_6/k_{-5}$ and $k_6/k_{-5} = k_4/k_1$ and setting $k_{-5} = 10k_5$ (based on the modeling with program Extend). Although the value of $k_4$ for $Et_3$-PAuSATg could not be determined due to $Et_3PO$ formation, it is reasonable to expect the less bulky ethyl complex to exchange more rapidly than $i\text{Pr}_3$PAuSATg (and therefore to have a larger $k_4$ value), since the bulkier *i*Pr groups provide more steric hindrance to reaction at Cys-34. A family of curves for various values of $k_4$, starting at $1.2 \times 10^2$ M$^{-1}$ s$^{-1}$, was generated Figure 6. Values of $k_4$ greater than $6 \times 10^2$ M$^{-1}$ s$^{-1}$ reproduce the experimentally determined $k_1^{obs}$ values for $[Et_3PAuSATg]$ well below the region where its concentration is in pseudo first-order excess of the albumin. Only at auranofin concentrations below those examined here, do the reaction rates decrease and become second order. The ability to reproduce the data when $[R_3$-PAuSATg] is the limiting reagent, as well as when it is in excess, provides strong support for the mechanism of eqs 11−13. An alternative, but less satisfactory, mechanism that predicts only a first order reaction for the Penefsky column data is given in the Appendix.

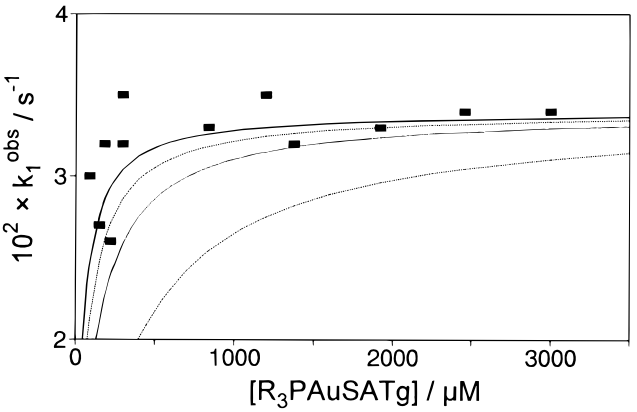


**Figure 6.** Computer fitting of the auranofin $k_1^{obs}$ values (■) to eq 21, using $k_5 = 3.4 \times 10^{-2}$ s$^{-1}$; $k_{-5} = 10k_5$ with $k_6$ chosen so that $k_4$ (=$k_5k_6/k_{-5}$) values are 960 (−), 600 (- - -), 360 (•••), and 120 (− •−) M$^{-1}$ s$^{-1}$.

The binding of gold in 1:1 ratio to total albumin when auranofin is in excess of the mercaptalbumin content (Figure 2) is a novel result that was unexpected in light of previous chromatographic studies.[9,15,17] It is the first evidence for an auranofin adduct, AlbSSR−$Et_3$PAuSATg (eq 7) other than AlbSAuPE$t_3$ (eq 1) and AlbS(AuPE$t_3$)$_2^+$ formed by ligand exchange at Cys-34. Its formation finds support in the report of Dhubhghiall *et al.* that ATgSH can bind hydrophobically to albumin.[13] The Hummel−Dreyer chromatographic results (Figure 3), obtained with the albumin−auranofin complex and excess auranofin in equilibrium throughout the elution process, confirm the Penefsky column data, where the rapidity of the separation precludes extensive dissociation. Conventional gel exclusion columns are eluted slowly (10 min−2 h, depending on column volume and length). Thus, any intact auranofin bound to the albumin Cys-34 disulfide species can dissociate during the separation, which explains why this additional binding mode was not observed previously.[9,11−13,15] Alternative auranofin binding sites at one or both of the drug sites in domains II and III can be eliminated, because populating them would lead to 1.6 or 2.6 Au/$Alb_{TOT}$ in contradiction of the 1.0 ratio found here. It is noteworthy that the 10−15 s required for the protein to elute over the Penefsky columns is less than 1 half-life for the albumin crevice-opening process of eq 11 ($t_{1/2} \approx 24$ s). If the crevice with intact auranofin molecules opens at a similar rate and if not every opening leads to diffusion of auranofin from the crevice, exactly the observed result, retention of auranofin in the crevice during passage over a Penefsky column, would be expected. The fact that dissociation of

(41) Bryan, D. L. B.; Mikuriya, M.; Hempel, J. C.; Melinger, D.; Heshim, M.; Pasternack, R. A. *Inorg. Chem.* **1987**, *26*, 4180−4185.
(42) Christodoulou, J.; Sadler, P. J.; Tucker, A. *Proc. 3rd International Conference on Gold and Silver in Medicine* in *Metal Based Drugs* **1994**, *1*, 527.

AlbSSR−$Et_3$PAuSATg is not instantaneous supports the assumption in the mechanism of eqs 11−13 that ATgSH displacement of $Et_3PAu^+$ (eq 12, reverse direction) is also preceded by a protein opening (eq 13, reverse direction) analogous to the forward direction of eq 11.

The rapid reaction of auranofin with the albumin Cys-34 residue is significant for the pharmacology of the drug. The studies described here employed physiological pH and protein concentrations (~600 $\mu$M albumin) close to those found *in vivo*. The clinically observed auranofin concentrations in serum, 10−25 $\mu$M, fall below the region of apparent first order reactions in Figure 6. Therefore, the *in vivo* reaction will be second order and governed by the rate constant $k_4$:

$$\text{rate} = k_4[\text{AlbSH}][\text{Et}_3\text{PAuSATg}] \qquad (23)$$

Since the AlbSH concentration is ~400 $\mu$M, which places it in large excess over the auranofin (a reversal of the experimental conditions), the reaction has a pseudo-first-order dependence on [$Et_3$PAuSATg]. Using a $k_4$ value of $8 \pm 2 \times 10^2$ $M^{-1}$ $s^{-1}$ estimated from Figure 6, a half-life can be calculated as $t_{1/2} = \ln 2/\{k_4[\text{AlbSH}]\} \approx 2$ s. Rapid displacement of ATgSH from auranofin by albumin according to the stoichiometry of eq 1 and the short half-life implied by eq 23 are consistent with the observation that 80% of the gold but only 10% of the thiolate from auranofin is observed in the blood after 20 min.[2] This facile conversion of auranofin to an albumin−gold metabolite also has important consequences for mechanism of action studies. Since $R_3PAu^+$ bound to Cys-34 is kinetically restricted in the pocket and thermodynamically more tightly bound than to the ATgSH ligand of the drug itself, it is less readily available to other potential binding sites and mechanistic targets. This is dramatically confirmed by the findings that the uptake, cytotoxicity, and antitumor potency of auranofin and the analogue (triphenylphosphine(8-thiotheophyllinato)gold(I) ($Ph_3$-PAuTtp) in macrophage and tumor cell cultures are systematically reduced by increasing concentrations of fetal calf serum, in which albumin is the principle gold binding site.[43−45] Future studies of cellular phenomena, enzyme inhibition, and biological processes can more realistically mimic *in vivo* conditions with albumin−gold complexes, such as AlbSAuPE$t_3$,[9] AlbSAuSTm,[46] and AlbSAuSG (GS = glutathione),[9] replacing the short-lived drug auranofin.

## Appendix

An alternative mechanism that predicts only first-order reactions under the Penefsky chromatography consitions is the following:

$$\text{AlbSX} + \text{R}_3\text{PAuSATg} \underset{k_{-8}}{\overset{k_8}{\rightleftharpoons}} \text{AlbSX}-\text{R}_3\text{PAuSATg} \qquad (24)$$

$$\text{AlbSH}-\text{R}_3\text{PAuSAT}_\text{g} \underset{k_{-9}}{\overset{k_9}{\rightleftharpoons}} {}^*\text{AlbSH}-\text{R}_3\text{PAuSAT}_\text{g} \qquad (25)$$

$${}^*\text{AlbSH}-\text{R}_3\text{PAuSATg} \underset{k_{-10}}{\overset{k_{10}}{\rightleftharpoons}} \text{AlbSAuPEt}_3 + \text{ATgSH} \qquad (26)$$

The initial step is rapid equilibrium binding of $R_3$PAuSATg to all forms of the protein ($K_8 = k_8/k_{-8} \gg 1$), eq 24, to form an adduct. The next step, eq 25, is a conformational change of the mercaptalbumin-containing adducts. The forward rate constant $k_9$, corresponds to crevice opening and/or Cys-34 configurational change[14] and is rate-determining. This rearrangement is followed by a rapid, intramolecular transfer of $R_3$-PAuSATg from its initial binding site to Cys-34 where the tetraacetylthioglucose ligand is displaced, eq 26. The bound $R_3$PAuSATg must be in close proximity to Cys-34 and able to transfer to it more rapidly than excess free $R_3$PAuSATg (up to 20-fold in some experiments) can migrate into the crevice. The concentrations of the initial adduct, AlbSH−$R_3$PAuSATg, and the final product, AlbSAu$PR_3$, are limited to the same extent by the lesser of the gold or protein concentrations.

By assuming complete formation of AlbSH−$R_3$PAuSATg and using the steady-state approximation for the conformationally altered adduct, [*AlbSH−$R_3$PAuSATg], one can derive the following rate law:

$$\text{d[D]/d}t = k_{10}\{(k_9[\text{AB}] + k_{-10}[\text{C}][\text{D}])/(k_{-9} + k_{10})\} - k_{-10}[\text{C}][\text{D}]$$

As in the earlier mechanism, A is AlbSH, B is $R_3$PAuSATg, C is AtgSH, and D is Alb$SAuPR_3$. AB and *AB represent the adduct in its normal and conformationally activated states.

If $k_{10} \gg k_{-9}$, then the expression simplifies to $k_9$[AB], and the observed rate constants $k_{1,\text{obs}}$ for auranofin and its isopropyl analogue equal $k_9$, the rate of crevice opening or Cys-34 rearrangement of the adduct. An alternative derivation, also starting from the rate law shown but avoiding the assumption that $k_{10} \gg k_{-9}$, argues that, under the chromatography conditions, [C] and [D] are negligible, with the consequence that the expression simplifies to $(k_9k_{10}/(k_{-9} + k_{10})\}$[AB]. The observed rate constants, $k_{1,\text{obs}}$, are equal to $k_9k_{10}/(k_{-9} + k_{10})$. With either simplification, the reaction would be first order and totally independent of the auranofin/albumin ratios.

In this mechanism, the reverse reaction of the NMR experiment corresponds exactly to the reverse direction of eq 26, and the experimental second-order rate constant $k_{-4}$, with dependence on AtgSH and AlbSAuPR3 equals $k_{-10}$. The preequilibrium of eq 24 is consistent with (1) the retention of $Et_3$PAuSATg in excess of Cys-34 during Penefsky and Hummel−Dryer chromatography experiments and its loss during conventional chromatography and (2) the small but reproducible changes for $^{31}$P NMR chemical shifts observed for "free" $R_3$-PAuX species in albumin solutions.[17] This mechanism can also explain the small, and possibly significant, differences in the two $k_1$ values, $3.4 \times 10^{-2}$ and $1.4 \times 10^{-2}$ $s^{-1}$, where R is Et and *i*Pr, since $R_3$PAuSATg is protein-bound before the rate-determining step.

Unfortunately, eqs 24−26 provide no explanation for the NMR results in the forward direction, where a rapid, second-order reaction is observed. They predict the same first-order reacton and rate constant under the NMR conditions and Penefsky chromatography conditions. One requries, therefore, and additional mechanism for $R_3$PAuSR exchange under the NMR conditons:

$$\text{AlbSH}-\text{R}_3\text{P}^{\ddagger}\text{AuSATg} + \text{ATgSH} \underset{k_{-11}}{\overset{k_{11}}{\rightleftharpoons}} \text{AlbSH}-\text{ATgSH} + \text{R}_3\text{P}^{\ddagger}\text{AuSATg} \qquad (27)$$

$$\text{AlbSAuPR}_3 + \text{ATgSH} \underset{k_{10}}{\overset{k_{-10}}{\rightleftharpoons}} {}^*\text{AlbSH}-\text{R}_3\text{PAuSATg} \qquad (28)$$

(43) Mirabelli, C. K.; Johnson, R. K.; Sung, C. M.; Faucette, L.; Muirhead, K.; Crooke, S. T. *Cancer Res.* **1985**, *45*, 32−39.
(44) Snyder, R. M.; Mirabelli, C. K.; Crooke, S. T. *Biochem. Pharmacol.* **1986**, *35*, 923.
(45) Arizit, M. P.; Garcia-Orad, A.; Sommer, F.; Silvestro, L.; Massiot, P.; Chevallier, P.; Gutierrez-Zorrilla, J. M.; Colacio, E.; Martinez de Pancorbo, M.; Tapiero, H. *Anticancer Res.* **1991**, *11*, 625−628.
(46) Shaw, C. F., III; Schaeffer, N. A.; Elder, R. C.; Eidsness, M. K.; Trooster, J. M.; Calis, G. H. M. *J. Am. Chem. Soc.* **1984**, *106*, 3511−3521.

$$R_3P^{\ddagger}AuSATg + *AlbSH{-}R_3PAuSATg \underset{k_{-12}}{\overset{k_{12}}{\rightleftharpoons}} AlbSAuP^{\ddagger}R_3 + R_3PAuSATg + ATgSH \quad (29)$$

$$AlbSH{-}ATgSH + R_3PAuSATg \xrightarrow{\text{fast}} AlbSH{-}R_3PAuSATg + ATgSH \quad (30)$$

The phosphine in AlbSH−$R_3$PAuSATg is spin-saturated (‡) during the NMR experiment in the forward direction, and then in eq 27 is displaced by the excess acetylthioglucose used to establish the equilibrium of Cys-34-bound and "free" gold. The acetylthioglucose also reacts with AlbSAu$Pr_3$, eq 28, to generate the activated adduct; this reaction is the reverse of eq 26 in the first part of the mechanism and hence the rate constant is $k_{-10}$. The activated adduct then reacts rapidly with $R_3$PAuSATg with unsaturated spin. If first step is rate-limiting, $k_{11}$ can be equated with the observed rate constants, $k_{3,obs}$ of the NMR experiments. These observed rate constants are proportional to $[AtgSH]_{eq}$, Figure 7 (as well as to $[AlbSH]_{eq}$, Figure 5, since both increase as excess AtgSH is added). The plot yields a second-order rate constant of 19 $M^{-1}$ $s^{-1}$ with an intercept, designated $k_9'$, which should correspond to the first-order exchange described by $k_9$ and in fact has the same order of magnitude:

$$k_{3,obs} = k_{11}[AB][ATgSH] + k_9'[AB]$$

The value of $k_{-10}$ (39 $M^{-1}$ $s^{-1}$) is not sufficiently larger than $k_{11}$ and the final step, eq 29, is expected from inorganic model studies[7,41] to be quite rapid.

While eqs 27−29 qualitatively account for the more rapid exchange observed in the NMR experiments, they have quantitative shortcomings. The agreement of $k_9'$ ($6 \times 10^{-2}$ $s^{-1}$) and $k_9 = k_{1,obs}$ ($1.4 \times 10^{-2}$ $s^{-1}$) is only to the correct order of magnitude. The value of $k_{-10}$ (39 $M^{-1}$ $s^{-1}$) is not sufficiently larger than $k_{11}$ to argue that the former is completely rate-determining. Other mechanisms considered for the rapid exchange of the NMR experiments and consistent with eqs 24−26 yielded incorrect predictions for albumin or acetylthioglucose dependence of the reactions when considered in detail.

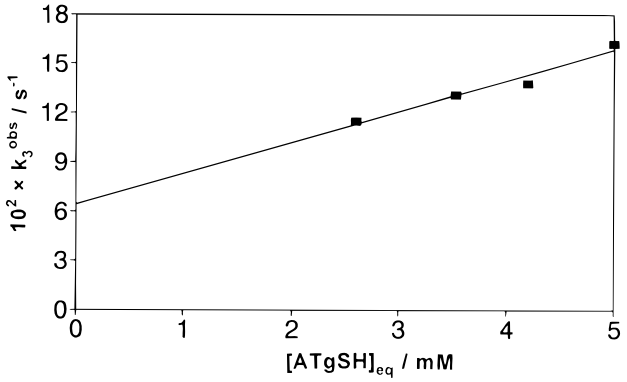


**Figure 7.** Dependence of $k_3^{obs}$ on $[AtgSH]_{eq}$. The observed rate constants for the forward reaction in the NMR experiments have been plotted to demonstrate that they also have a linear dependence on [AtgtSH], with a second-order rate constant of 19 $M^{-1}$ $s^{-1}$ and a finite intercept of $6 \times 10^{-2}$ $s^{-1}$.

For these reasons and because eqs 24−29 constitute an *ad hoc* explanation, the simple, elegant mechanism of eqs 11−13 in the Discussion remains intellectually more compelling. Further research may reveal mechanistic details that refine eqs 11−13, but no mechanism will change the key experimental facts that (1) the initial reactions follow slow, first-order kinetics, while (2) the exchange under NMR conditions is faster and second order. Thus, an initial, slow, albumin-centered step governing net product formation and multiple exchanges at an accessible Cys-34 under equilibrium (NMR) conditions are required in any more sophisticated mechanism.

**Acknowledgment.** We thank Dr. Eugene DeRose for his assistance with the design and execution of the NMR experiments. We thank Dr. James Hoeschele (presently at the Michigan State University) for his generous gift of *i*$Pr_3$PAuCl and *i*$Pr_3$PAuSATg and Dr. David Hill of Smith Kline and French for providing $Et_3$PAuCl and $Et_3$PAuSATg, as well as for stimulating discussions of gold biochemistry. C.F.S. thanks the Deutsches Forschungsgemeinschaft for a Gastprofessonship for 1993−1994 and the Medizinisches Institut für Umwelthygiene, Düsseldorf, for its hospitality.

IC9414280